ACS PHYSICAL CHEMISTRY Au
AN OPEN ACCESS JOURNAL OF THE AMERICAN CHEMICAL SOCIETY

pubs.acs.org/physchemau

Article

Estimating the Single-Element Concentration of Intercalated Insulators for the Emergence of Superconductivity

Shermane M. Benjamin*

Cite This: *ACS Phys. Chem Au* 2022, 2, 108–117

Read Online

ACCESS | Metrics & More | Article Recommendations | Supporting Information

ABSTRACT: To predict whether a compound will superconduct and to predict its transition temperature T_c prior to measurement have always been desires of the materials science community. Matthias was first to report the necessary conditions for the occurrence of superconductivity in elements, compounds, and alloys in terms of density (valence electrons per atom). This current report is motivated by somewhat similar empirical observations concerning the importance of valence electrons per unit cell; more specifically, dopant valence electrons per unit cell within intercalated insulators. In this article, though not exhaustive, a representative list of 40 superconductors will be used to show that the onset of superconductivity (insulator–superconductor boundary) within intercalated insulators can easily be modeled, almost exactly, by the ideal gas law equation. Given this observation, in contrast to Matthias, interactions are semiclassically accounted for to ultimately determine the single-element onset concentration needed to bring about superconductivity within many intercalated insulators known to date. The 13 compounds which were previously intercalated and will be discussed include inorganics, $TiSe_2$, C_{60}, $YBa_2Cu_3O_6$, $IrTe_2$, Bi_2Se_3, MoS_2, ZrNCl, HfNCl, BP (black phosphorus), $HoTe_3$, and Y_2Te_5, and organics, $C_{22}H_{14}$ and $C_{14}H_{10}$. In essence, the overall objective of this report is to offer a slightly different viewpoint on superconductivity, led by empirical observations, which seemingly leads to predictable experimental outcomes. If newly discovered materials further validate this approach to intercalated superconductors, with minor refinements, a route to purposefully designing superconductors may be accessible through onset conditions outlined in this article.

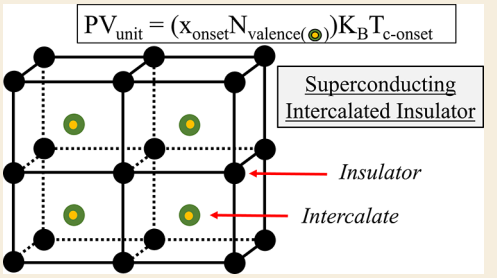

KEYWORDS: *intercalation, insulator, superconductivity, ideal gas law, Mott insulator, semiconductor, predicting T_c, Matthias rules*

INTRODUCTION

Since the discovery of the first superconductor, Hg,[1] countless efforts have been made to arrive at a theory leading to the necessary conditions for superconductivity to emerge within a given system.[2] To date, current predictions and their reliance on easily accessible parameters for experimentalists (e.g., valence electrons per atom, atomic radius, and atomic volume) are heavily influenced by the works of Matthias and others.[3,4] Without strictly considering interactions, it was found empirically that superconductivity generally occurred if the average number of valence electrons per atom is greater than two but less than eight (i.e., $2 < N_{ave}/\text{atom} < 8$) for elements, compounds, and alloys. Within these limits for elemental superconductors of the same column of the periodic table, the transition temperature was discovered to be proportional to the product of the radius R and the inverse mass M of the neutral atom, $T_c \sim R^{18}/M$. What is remarkable is that an oversimplification of superconductivity, by neglecting the interactions inside superconductors, gives rise to fundamental qualitative results for most materials in the superconducting state. In contrast, the aim of this report is to examine the insulator–superconductor boundary of intercalated insulators via Coulomb interactions for quantitative predictions.

Coupled with the works of Matthias and others,[5] modern advances in computing power and programing have allowed machine learning algorithms to join the race in discovering new superconducting compounds.[6,7] These methods usually rely on the chemical composition and properties of the periodic table, variables of easy access to materials scientists and chemists. Lists of possible superconductors are often produced along with physical and chemical parameters, which are weighted heavily during the prediction stage (e.g., valence electrons[6]), giving clues to the most probable variables of importance to induce superconductivity. In fact, superconductors $CaBi_2$ and $Hf_{0.5}Nb_{0.2}V_2Zr_{0.3}$ were discovered via machine learning.[7] They were discovered without prior knowledge of their existence as they were not a part of the public database used by the algorithm. Though some aspects of this technique lead to successful predictions more than half of the time (e.g., predicting T_c),[7] they do not give rise to convenient equations that can be manipulated

Received: September 6, 2021
Revised: October 18, 2021
Accepted: November 4, 2021
Published: November 16, 2021

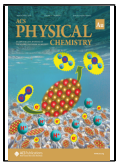

https://doi.org/10.1021/acsphyschemau.1c00027
ACS Phys. Chem Au 2022, 2, 108–117

Table 1. Onset Transition Temperatures of Superconducting Intercalated Insulators[a]

[ref.]compound	$T_{c\text{-}exp.onset}$ (K)	$T_{c\text{-}PV} = PV_{unit}/(xN_{val}K_B)$	N_{val}	$x_{exp.onset}$	V_{unit} (Å^3)	BCS
[8] Cu_xTiSe_2	1	0.96	11[b]	0.045	65	Y
[16] Pd_xTiSe_2	1.8	0.42[c]	10[b]	0.11	65	?
[17] Cu_xIrTe_2	1.25	1.00	11[b]	0.05	75	N
[15] $Nb_xBi_2Se_3$	2.5	2.50	5[b]	0.25	426	N
[18] $Sr_xBi_2Se_3$	2.8	15.6[c]	2	0.1	426	N
[19] $Cu_xBi_2Se_3$	2.7	2.81	11[b]	0.1	426	N
[20,21] $K_{2+x}C_{60}$	19.5	20.26	1	1	2810	Y
[21] $Rb_{2+x}C_{60}$	30 (saturates@23)	20.26	1	1	2810	Y
[22] $Cs_{2+x}C_{60}$	30[d] (saturates@20)	20.26	1	1	2810	Y
[23] Na_xMoS_2	3.6	3.74	1	0.3	153	Y
[24,25] K_xMoS_2	7	8.02	1	0.13	142	Y
[26] Rb_xMoS_2	6.25[d]	3.74[c]	1	0.3	153	Y
[26] Cs_xMoS_2	6.3[d]	4.26	1	0.3	174	Y
[27] Ca_xMoS_2	4	3.51	2	0.2	191	Y
[27] Sr_xMoS_2	5.6	3.51	2	0.2	191	Y
[27] Ba_xMoS2	5.7	3.51	2	0.2	191	Y
[28] $K_{2+x}C_{22}H_{14}$	6.5	8.22	1	0.6	672	?
[28] $Rb_{2+x}C_{22}H_{14}$	6.9[d,e]	4.48	1	1.1	672	?
[29] $Ca_{1+x}C_{22}H_{14}$	7[d]	4.95	2	0.5	672	Y
[30] $K_{2+x}C_{14}H_{10}$	4.8[d,e]	3.56	1	1	485	?
[30] $Rb_{2+x}C_{14}H_{10}$	5[d,e]	3.56	1	1	485	?
[31] $Sr_{1+x}C_{14}H_{10}$	5.6 (saturates@4.8)	3.56	2	0.5	485	N
[31] $Ba_{1+x}C_{14}H_{10}$	5.4 (saturates@4.8)	3.56	2	0.5	485	N

[a]Table includes experimentally measured superconducting transition temperature $T_{c\text{-}(exp.onset)}$, empirically observed $T_{c\text{-}PV} = (PV_{unit})/(x_{exp.onset}N_{val}K_B)$, and physical properties to calculate T_{c-PV} for intercalated insulators. P = 1 atm for all compounds. [b]N_{val} includes outer s and d electrons for transition metals. [c]Calculated temperature deviates considerably from the experimentally determined value. [d]No available detailed reports on efforts to obtain lower concentrations. Therefore, lower concentrations might be possible, effectively increasing calculated $T_{c\text{-}PV}$. [e]The emergence of superconductivity depends on the synthesis time, non-monotonically, for some alkali-intercalated organics.[28] Only synthesis at t = 20 h was attempted for $Rb_{2+x}C_{14}H_{10}$, and similarly for others.[30] Therefore, $x_{exp.onset} < 1$ might be possible.

to create or modify superconductors predictably. Despite this shortcoming, machine learning still provides a useful computational tool in the search for new superconductors.

To arrive at a better understanding of the onset of superconductivity at the insulator−superconductor boundary, doped insulators serve as ideal candidates for synthesis and characterization as they enable a perturbative perspective on this issue. The ability to monitor these systems (e.g., via resistance, $R(T)$) as they gradually become metallic superconductors through doping has allowed better quantification of the necessary parameters governing the boundary between the two distinct electronic states. Superconducting intercalates such as Cu_xTiSe_2,[8] $Alkali_3C_{60}$ (Alkali = K, Rb, and Cs),[9−11] and $YBa_2Cu_3O_{6+x}$[12] represent some examples, where only specific combinations of dopant parameters (e.g., radius, charge, concentration, and so forth) bring out superconductivity from their insulating counterparts $TiSe_2$, C_{60}, and $YBa_2Cu_3O_6$, respectively. Incidentally, these compounds also span the gamut of known superconductors to date. Intercalates Cu_xTiSe_2, $Alkali_3C_{60}$, and $YBa_2Cu_3O_{6+x}$ are low-temperature (∼2 K) layered BCS,[13] mid-temperature (∼30 K) non-BCS, and high-temperature (∼90 K) non-BCS superconductors, respectively, where "BCS" indicates the microscopic theory of superconductivity developed by Bardeen, Cooper, and Schrieffer.[14] As a result, this report will address these specific intercalates, along with 37 other superconducting intercalated insulators known to date.

$$PV_{unit} = (x_{onset}N_{val}) \times K_B T_{c\text{-}exp.onset} \quad (1)$$

The following is a summary for the remainder of the article. First, eq 1 is shown to be the empirical equation governing the onset of superconductivity in intercalated insulators, considering the significance of intercalate valence electrons, where P, V_{unit}, $x_{exp.onset}$, N_{val}, K_B, and $T_{c\text{-}exp.onset}$ are the pressure, unit cell volume, experimentally measured dopant concentration at the onset of superconductivity, number of valence electrons in dopants (including s and d electrons for transition metals), Boltzmann constant, and experimentally measured superconducting temperature at $x_{exp.onset}$, respectively. Keep in mind that the onset transition temperature is not necessarily at the optimum doping usually associated with maximum T_c. Given the form of eq 1, a description for intercalated insulators exhibiting superconductivity, in terms of Coulomb energies near the Fermi energy, will be developed and tested. These ideas will be mapped first to Cu_xTiSe_2 to determine the value of one unknown dimensionless quantity, A_s. After that the onset concentration required to induce superconductivity in known intercalated organic and inorganic insulators will be calculated, given the easily acquired physical parameters of the host and the intercalate. Calculated values will then be compared to those reported from experiment.

Intercalated Insulators: $T_{c\text{-}exp.onset} \approx PV_{unit}/(x_{exp.onset}N_{val}K_B)$

As certain insulators are increasingly intercalated with specific dopants (e.g., Bi_2Se_3 doped with Nb), at a critical concentration, $x_{exp.onset}$, superconductivity can be observed. Some possess phase diagrams with many superconducting phases such as $YBa_2Cu_3O_{6+x}$ ($0.35 < x < 1$), while others do not (e.g., $Nb_{0.25}Bi_2Se_3$[15]). All of these systems seem to obey eq 1 with regard to their onset concentrations. Data for the experimentally

https://doi.org/10.1021/acsphyschemau.1c00027
ACS Phys. Chem Au 2022, 2, 108−117

Table 2. Onset Transition Temperatures of Superconducting Intercalated Insulators[a]

[ref.]compound	$T_{c\text{-}exp.onset}$ (K)	$T_{c\text{-}PV} = PV_{unit}/(xN_{val}K_B)$	N_{val}	$x_{exp.onset}$	V_{unit} (Å^3)	BCS
[32] Li_xZrNCl	15 (saturates @ 8)	14.26	1	0.16	311	N
[32] Na_xZrNCl	15	8.46[c]	1	0.27	311	N
[32] K_xZrNCl	15	10.89	1	0.21	311	N
[33] Mg_xZrNCl	15 (saturates@11)	11.42	2	0.1	311	N
[34] Zn_xZrNCl	14[d](saturates@5)	4.76	12[b]	0.04	311	N
[35] Li_xHfNCl	20 (saturates@15)	15.19	1	0.16	331	N
[36] Na_xHfNCl	22 (saturates@12)	13.50	1	0.18	331	N
[33] Mg_xHfNCl	25 (saturates@15)	12.15	2	0.1	331	N
[37] Sr_xHfNCl	20.3 (saturates@15)	13.50	2	0.09	331	N
[37] Ba_xHfNCl	20.2 (saturates@10)	12.15	2	0.1	331	N
[38] K_xBP	3.8	5.58	1	0.2	152	Y
[38] Rb_xBP	3.8	5.58	1	0.2	152	Y
[38] Cs_xBP	3.8	5.58	1	0.2	152	Y
[38] Ca_xBP	3.8	5.58	2	0.1	152	Y
[39] Pd_xHoTe3	2.85	4.27	10[b]	0.08	465	Y
[39] $Pd_xY_2Te_5$	2.85	4.27	10[b]	0.08	465	Y

[a]continued. [b]N_{val} includes outer s and d electrons for transition metals. [c]Calculated temperature deviates considerably from experimentally determined value. [d]No available detailed reports on efforts to obtain other concentrations.

measured superconducting transition temperature $T_{c\text{-}exp.onset}$ and the empirically observed $T_{c\text{-}PV} = (PV_{unit})/(x_{exp.onset}N_{val}K_B)$ are compared in Tables 1 and 2. Equation 1 holds regardless of the temperature range of superconductivity. The relation even satisfies both BCS and non-BCS superconductors. This observation is likely not due to coincidence as eq 1 only applies to single-element intercalated insulators, which show superconductivity; no other type of doped superconductor closely obeys this relation, except perhaps low-density semimetals like $IrTe_2$.

The equality between $T_{c\text{-}exp.onset}$ and $T_{c\text{-}PV}$ implies the onset of superconductivity in intercalated insulators, and its associated transition temperature can be expressed without the isotopic mass. While in opposition to Matthias' findings (e.g., $T_c \sim R^{18}/M$), keep in mind that the realization of the ideal gas law relation is made specifically at the insulator−superconductor boundary. It is not a general feature of superconductors away from the boundary. The ideal gas relation is shown graphically in Figure 1 for all compounds in Tables 1 and 2. It displays a plot of inverse onset transition temperature, $1/T_{c\text{-}exp.onset}$, versus electron density, N_{ave}/V_{unit}. Here, the electron density is defined as the average number of intercalating valence electrons, $N_{ave} = x_{exp.onset}N_{val}$, per unit cell volume, V_{unit}. The ideal gas slope at 1 atm ± 20% (i.e., the pressure used in experiments for all compounds) passes through the data despite a handful of outliers. Errors arising from experimentally determined onset concentrations and onset temperatures were either unreported or within the range of 3% to approximately 20%.

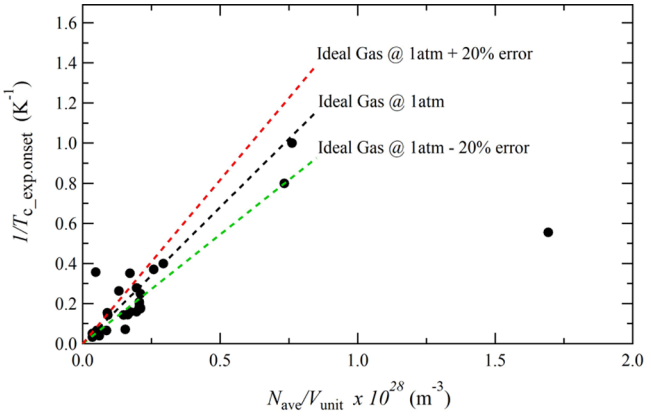

Figure 1. Inverse onset transition temperature $(1/T_{c-exp.onset})$ versus intercalate valence electron density (N_{ave}/V_{unit}) for all 39 compounds listed in Tables 1 and 2. Black, red, and green dashed lines represent fit of the ideal gas law equation at 1 atm, at 1 atm + 20% error, and at 1atm − 20% error, respectively.

Note the form of eq 1 suggests "external" energy $(E_{ext} = PV_{unit})$ is equal to the energy within the unit cell $(E_{in} = x_{onset}N_{val}K_BT_{c-onset})$, at the onset of superconductivity for intercalated insulators. E_{ext} can be calculated, so the latter is where the author offers an interpretation of $T_{c-onset}$. For E_{in}, in terms of Coulomb interactions involving valence electrons, in general, the energy within a doped unit cell (empirically proportional to $K_BT_{c-onset}$) can be described as shown in eq 2; where prime denotes the host. Essentially, eq 2 says the total energy from electron−electron interactions (ee) and electron−proton interactions (ep) is a result of three main interactions within the unit cell: dopant−dopant $(E_{ep} + E_{ee})$, dopant−host $(E_{e'p} + E_{p'e} + E_{e'e})$, and host−host $(E_{e'p'} + E_{e'e'})$.

$$\text{Coulomb interactions} = (E_{ep} + E_{ee}) + (E_{e'p} + E_{p'e} + E_{e'e}) + (E_{e'p'} + E_{e'e'}) \quad (2)$$

For intercalated insulators, host−host interactions $(E_{e'p'} + E_{e'e'})$ do not contribute to the metallic state as all hosts are insulators in this report; therefore, $E_{e'p'} + E_{e'e'} = 0$. This report will also neglect dopant−host interactions $(E_{e'p} + E_{p'e} + E_{e'e})$, admittedly because they are difficult to model, and second, because intercalation is a comparatively weaker[40] form of bonding in relation to ionic and covalent bonds. However, considering dopant−host interactions could prove unavoidable for compounds doped under particle exchange (e.g., $La_{2-x}Ce_xCuO$[41]). Thus, dopant−host interactions, especially in weakly intercalated compounds, will be ignored but is understood to be non-zero in general. Upcoming sections will show that modeling only intercalate−intercalate interactions $(E_{ep} + E_{ee})$, near the Fermi energy, is sufficient to approximate

https://doi.org/10.1021/acsphyschemau.1c00027
ACS Phys. Chem Au 2022, 2, 108−117

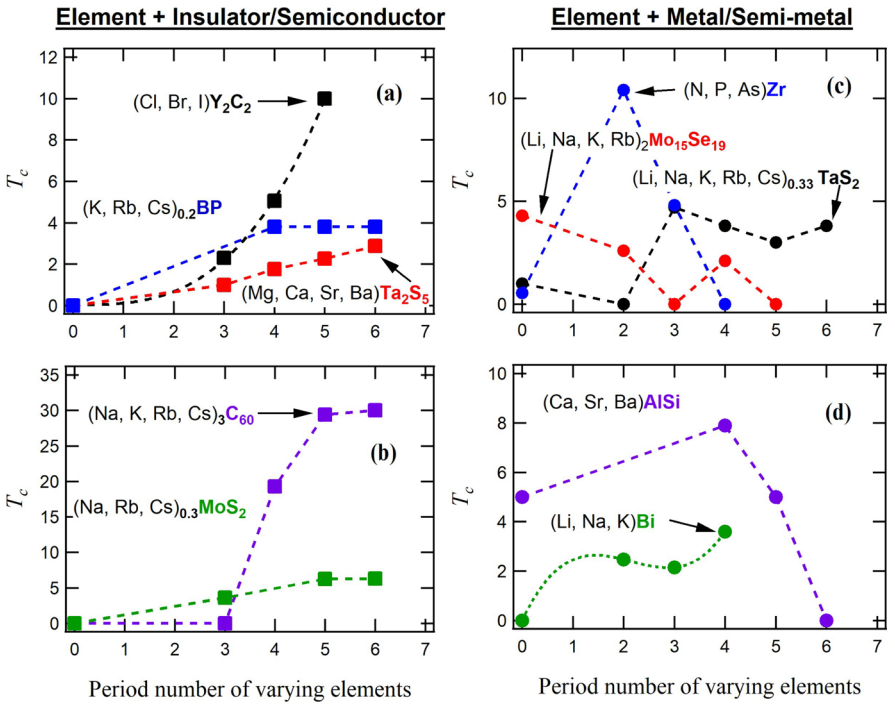

Figure 2. Period number of varying elements versus T_c. Plots (a,b) are the result of incorporating elements of the same group of the periodic table, in increasing period number, into five insulating/semiconducting solids. Compounds displayed are (Cl, Br, I)Y_2C_2, (K, Rb, Cs)$_{0.2}$BP, (Mg, Ca, Sr, Ba)Ta_2S_5, (Na, K, Rb, Cs)$_3C_{60}$, and (Na, Rb, Cs)$_{0.3}MoS_2$.[23,25−27,38,42,46−51] Pristine insulating/semiconducting compounds are denoted with period number = 0 and T_c = 0. A monotonic increase in T_c to saturation is observed when elements are incorporated into non-metallic solids with increasing period number. Plots (c,d) are the result of incorporating elements of the same group of the periodic table, in increasing period number, into five metallic/semimetallic solids. Compounds displayed are (Li, Na, K, Rb, Cs)$_{0.33}TaS_2$, (N, P, As)Zr, (Li, Na, K, Rb)$_2Mo_{15}Se_{19}$, (Mg, Ca, Sr, Ba)AlSi, and (Li, Na, K)Bi.[52−57] Pristine, unincorporated metallic/semimetallic compounds are denoted with period number = 0. A nonmonotonic, oscillatory-like behavior is observed when elements are incorporated into metallic/semimetallic solids with increasing period number. Unit cell volumes within each series of element−solid pairs are nearly identical. Transition temperatures for Zr compounds, AlSi, and LiBi were found in the SuperCon database.

the onset of superconductivity for many intercalated insulators known to date.

Microscopic Description of T_c(a, b, c, R_{atom}, and x_{onset})

As previously mentioned, the form of eq 1 is incredibly similar to the ideal gas law, $PV = NK_BT$. For an ideal gas, N is the number of free point-like particles within an enclosed volume V. The pressure, P, is a result of the random elastic motion of these free particles whose average velocities can be interpreted as temperature, T. The most probable reason for eq 1 having an "ideal gas"-like form is because it applies specifically to the limit of the lowest concentration ($(x_{onset}N_{val})/V_{unit}$), where superconductivity first arises in intercalated insulators. Since superconductivity can be modeled as a Fermi gas,[42] the ideal gas law relation is possibly realized as it is the classical limit to low-density (i.e., concentration) quantum gases. Though similar in form, there are two major differences between eq 1 and the ideal gas law. First, the former describes a particular number of dopant valence electrons, $x \times N_{val}$, within an insulating unit cell volume. Most of these electrons are not free to move classically throughout the host insulator's lattice because they are bound to the intercalate's nucleus; even though quantum mechanics requires them to be probabilistic and "gas-like" around their orbitals. Consequently, the second difference arises in the interpretation of temperature within eq 1. Instead of the temperature (i.e., internal energy) arising from an average velocity through elastic kinematic interactions (with other dopants and inner surface of volume) like a classical ideal gas, it is proposed that the temperature arises mostly from the Coulomb interactions involving intercalate valence electrons near the Fermi energy. With a semiclassical approach, these ideas will now be used to rewrite the right side of eq 1 in terms of Coulomb energies, $E_{Coulomb} = (q_1q_2\kappa_e)/(r)$, and the Fermi energy, where r is the distance separating charges q_1 and q_2, and κ_e is the Coulomb constant. These energies will eventually be a function of intercalate-dependent variables and the intercalate's spatial distribution (i.e., nearest-neighbor unit cells) throughout the host.

To account for only intercalate−intercalate Coulomb energies involving valence electrons, N_{val} is rewritten in terms of N_{ep} and N_{ee}. N_{ep} and N_{ee} in eq 3 represent the number of valence electrons interacting with the effective nuclear charge (nearest positive charge) of the intercalate and the number of valence electrons interacting with the nearest neighboring valence electrons, respectively. The total thermal energy for N_{val} in terms of K_BT in eq 1 can now be rewritten as the energy distributed over E_{ep}, E_{ee}, and E_{fermi} in eq 3, which are the Coulomb energy of the electron−proton interaction, Coulomb energy of the electron−electron interaction, and the Fermi energy relating to the nearly free electron model in three dimensions[43] for non-interacting electrons, respectively.

$$PV_{unit} = A_s \times |x \times (N_{ep}E_{ep} + N_{ee} \times (E_{ee} - E_{fermi}))|$$
$$, \text{ for } x = x_{onset}(x_{min}) \quad (3)$$

The constant A_s is introduced to normalize the thermodynamic energy PV_{unit} to the newly introduced Coulomb terms and the Fermi energy on the right-hand side of eq 3. The constant will be determined in the next section. Subsequently, if

https://doi.org/10.1021/acsphyschemau.1c00027
ACS Phys. Chem Au 2022, 2, 108−117

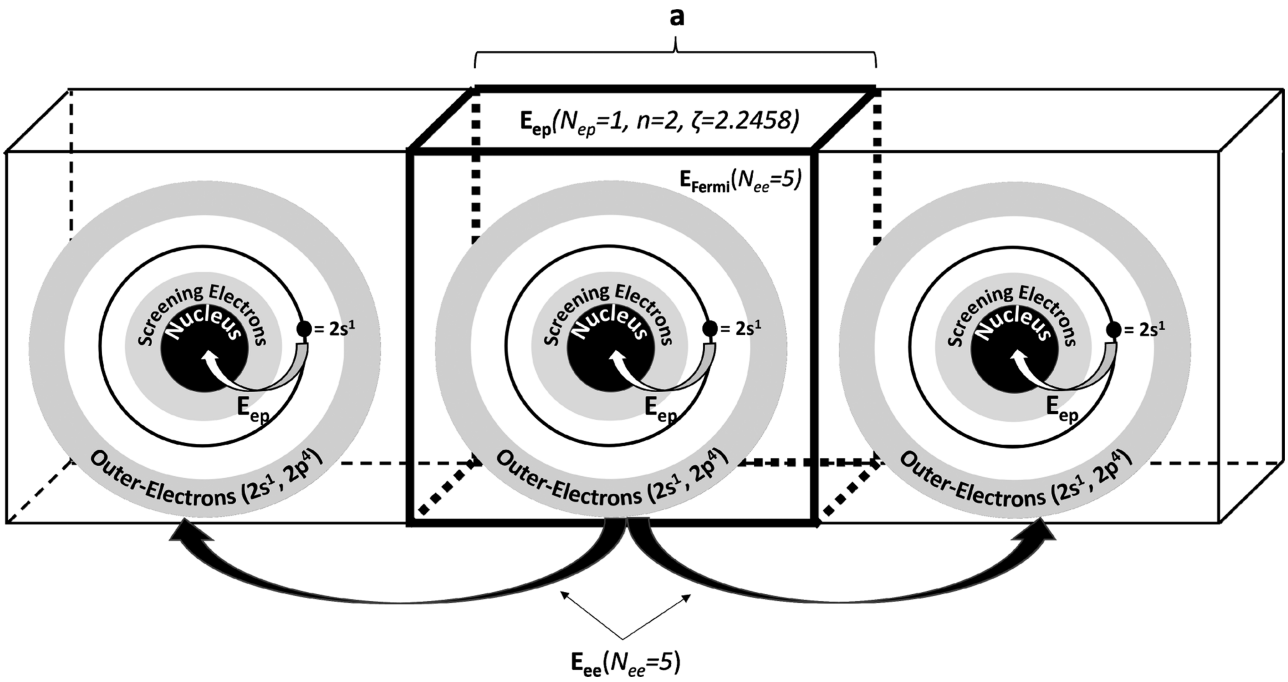

Figure 3. Oxygen intercalated within a generic volume. Image depicts one intercalated oxygen atom ($x = 1$) per unit cell within a generic volume along one dimension. The parts of the oxygen atom that are emphasized are the nucleus, screening electrons between the $2s^1$ electron (i.e., $N_{ep} = 1$, $n = 2$ and $\zeta = 2.245845$) and the nucleus, and outer electrons $2s^12p^4$ (i.e., $N_{ee} = 5$). Energies shown are the Fermi energy E_{Fermi} as a function of N_{ee}, the interaction energy E_{ep} between the $2s^1$ electron and the nucleus as a function of the effective nuclear charge $Z_{eff} = n \times \zeta$, and the interaction energy E_{ee} between the outer electrons of the nearest-neighboring unit cells along one direction/principal axis.

correct, numerically solving eq 3 for "x" should give the necessary minimum onset concentration to "turn on" superconductivity in single-element intercalated insulators. Such an outcome assumes all contributing energies are weighted equally at the onset.

The electron−proton interaction energy E_{ep} in eq 4 is a result of the effective nuclear charge, $q_2 = Z_{eff} \times e$, of the intercalate seen by its N_{ep} electrons ($q_1 = -xN_{ep} \times e$), where e is charge and R is the atomic radius of the intercalate. All atomic radii used within this report are the average between the empirical[44] and calculated[45] values, which differ at most by approximately 10%. The electron−electron interaction energy E_{ee} in eq 5 is a result of N_{ee} electrons ($q_2 = -xN_{ee} \times e$) interacting with the nearest neighboring intercalate N_{ee} electrons ($q_1 = -2xN_{ee}\sin(xN_{ee}\pi) \times e$) from all six neighboring unit cells along principal axes (lattice constants a, b, and c), thereby accounting for the "2" in eq 5.

The expected form of q_1, and consequently E_{ee}, is modulated by $\sin(xN_{ee}\pi)$ because of another empirical observation similar to one of Matthias' original discoveries. Matthias noticed that the transition temperature of solid solutions containing transition metals was an oscillatory function of density (valence electron per atom).[4,5] Figure 2 displays the current observation made for compounds derived from combining non-metals or metals with elements chosen from similar groups of the periodic table. Notice that the oscillatory behavior emerges only when elements are paired with "metals" (Figure 2c,d), with increasing period number, as opposed to non-metals (Figure 2a,b). In fact, systematically pairing non-metals with elements in increasing period number yields a monotonic increase in T_c to saturation. Increasing the period number of the varying element increases the atomic radius and weight, and the number of its valence electrons is unchanged. Larger radii inevitably elevates electron−electron interactions between these valence electrons and the free electrons already in metallic systems. Consequently, $\sin(xN_{ee}\pi)$ was chosen (as opposed to density, $\sim \sin(N_{ee}/V_{unit})$) to modulate E_{ee} as each family of compounds shares similar volumes, and because it seems only relevant when heightened electron−electron interactions are present in some form.

The Fermi energy E_{fermi} is in three dimensions in eq 6. It is a function of x, N_{ee}, V_{unit}, m_e, and $\hbar$. The latter two constants are the electron's rest mass and Planck's constant divided by 2π, respectively.

$$E_{ep} = -(xN_{ep})(Z_{eff})(e^2\kappa_e)\left(\frac{1}{R}\right) \tag{4}$$

$$E_{ee} = (xN_{ee})^2 \times 2\sin(\pi xN_{ee})(e^2\kappa_e)\left(\frac{1}{a} + \frac{1}{b} + \frac{1}{c}\right) \tag{5}$$

$$E_{fermi} = \frac{\hbar^2}{2m_e}\left(\frac{3\pi^2 xN_{ee}}{V_{unit}}\right)^{2/3} \tag{6}$$

Choosing N_{ep} and N_{ee} and Calculating Z_{eff}

There are now only two variables and one constant left to be determined in eq 3; they are N_{ee}, N_{ep}, and A_s, respectively. Electron−electron interactions are maximized in the metallic and superconducting states.[14,58] For this reason, the number of available valence electrons taking part in electron−phonon interactions is minimized to $N_{ep} = 1$ for all intercalates (e.g., the inner $2s^1$ electron within oxygen in Figure 3). Interaction energies E_{ep} and E_{ee} and the Fermi energy E_{Fermi} are depicted in Figure 3 for one oxygen atom intercalated at $x = 1$ within a generic volume along one dimension.

For intercalates from groups 13−17 of the periodic table and transition metals, $N_{ee} = N_{val} - 1$. For example, oxygen yields $N_{val} = 6$ and $N_{ee} = 5$ and copper yields $N_{val} = 11$ and $N_{ee} = 10$, where the latter "N_{val}" includes all the outer s and d electrons because it

https://doi.org/10.1021/acsphyschemau.1c00027
ACS Phys. Chem Au 2022, 2, 108−117

Table 3. Onset Concentration of Superconducting Intercalated Insulators[a]

[ref.]Compound	$x_{exp.onset}$	$x_{calc.onset}$	N_{ep}	N_{ee}	N_{val}	R (Å)	Z_{eff} [n, ζ]	V_{unit} (Å^3)
[16] Pd_xTiSe_2	0.11	0.1063	1	9	10[b]	1.545	13.618 [4d, 3.4044]	65
[17] Cu_xIrTe_2	0.05	0.0472	1	10	11[b]	1.4	13.201 [3d, 4.4002]	75
[15] $Nb_xBi_2Se_3$	0.25	0.2508	1	4	5[b]	1.715	11.238 [4d, 2.8094]	426
[18] $Sr_xBi_2Se_3$	0.1	0.3601[c]	1	2	2	2.095	11.932 [4p, 2.9830]	426
[19] $Cu_xBi_2Se_3$	0.1	0.1077	1	10	11[b]	1.4	13.201 [3d, 4.4002]	426
[20,21] $K_{2+x}C_{60}$	1	0.9662	1	1	1	2.315	7.7256 [3p, 2.5752]	2810
[21] $Rb_{2+x}C_{60}$	1	0.8593	1	1	1	2.5	10.881 [4p, 2.7202]	2810
[22] $Cs_{2+x}C_{60}$	1[d]	0.8129	1	1	1	2.815	13.651 [5p, 2.7302]	2810
[23,24] Na_xMoS_2	0.3	0.2149	1	1	1	1.85	6.8018 [2p, 3.4009]	153
[25,51] K_xMoS_2	0.13	0.2173[c]	1	1	1	2.315	7.7256 [3p, 2.5752]	142
[26] Rb_xMoS_2	0.3[d]	0.1966	1	1	1	2.5	10.881 [4p, 2.7202]	153
[23] Cs_xMoS_2	0.3[d]	0.199	1	1	1	2.815	13.651 [5p, 2.7302]	174
[27] Ca_xMoS_2	0.2	0.3365	1	2	2	1.87	8.6583 [3p, 2.8861]	191
[27] Sr_xMoS_2	0.2	0.2079	1	2	2	2.095	11.932 [4p, 2.9830]	191
[27] Ba_xMoS_2	0.2	0.1932	1	2	2	2.34	14.800 [5p, 2.9601]	191
[28] $K_{2+x}C_{22}H_{14}$	0.6	0.4936	1	1	1	2.315	7.7256 [3p, 2.5752]	672
[28] $Rb_{2+x}C_{22}H_{14}$	1.1[d,e]	0.4241[c]	1	1	1	2.5	10.881 [4p, 2.7202]	672
[29] $Ca_{1+x}C_{22}H_{14}$	0.5[d]	0.4391	1	2	2	1.87	8.6583 [3p, 2.8861]	672
[30] $K_{2+x}C_{14}H_{10}$	1[d,e]	0.4126[c]	1	1	1	2.315	7.7256 [3p, 2.5752]	485
[30] $Rb_{2+x}C_{14}H_{10}$	1[d,e]	0.3579[c]	1	1	1	2.5	10.881 [4p, 2.7202]	485
[31] $Sr_{1+x}C_{14}H_{10}$	0.5	0.3583	1	2	2	2.095	11.932 [4p, 2.9830]	485
[31] $Ba_{1+x}C_{14}H_{10}$	0.5	0.3359	1	2	2	2.34	14.800 [5p, 2.9601]	485
[12] $YBa_2Cu_3O_{6+x}$	0.35	0.1981	1	5	6	0.54	4.4916 [2s, 2.2458]	243

[a]Table includes experimentally measured onset concentration $x_{exp.onset}$ for superconductivity, calculated concentration $x_{calc.onset}$, and physical properties to compute $x_{calc.onset}$ for intercalated insulators. [b]N_{val} includes outer s and d electrons for transition metals. [c]Calculated concentration deviates considerably from experimentally determined value. [d]No available detailed reports on efforts to obtain lower concentrations. [e]The emergence of superconductivity depends on the synthesis time, non-monotonically, for some alkali-intercalated organics.[28] Only synthesis at t = 20 h was attempted for $Rb_{2+x}C_{14}H_{10}$, and similarly for others.[30] Therefore, $x_{exp.onset}$ <1 might be possible.

Table 4. Onset Concentration of Superconducting Intercalated Insulators[a]

[ref.]compound	$x_{exp.onset}$	$x_{calc.onset}$	N_{ep}	N_{ee}	N_{val}	R (Å)	Z_{eff} [n, ζ]	V_{unit} (Å^3)
[32] Li_xZrNCl	0.16	0.5439[c]	1	1	1	1.56	2.6906 [1s, 2.6906]	311
[32] Na_xZrNCl	0.27	0.3149	1	1	1	1.85	6.8018 [2p, 3.4009]	311
[32] K_xZrNCl	0.21	0.3333	1	1	1	2.315	7.7256 [3p, 2.5752]	311
[33] Mg_xZrNCl	0.1	0.3457[c]	1	2	2	1.475	7.8258 [2p, 3.9129]	311
[34] Zn_xZrNCl	0.04[d]	0.1022[c]	1	11	12[b]	1.385	5.9652 [4s, 1.4913]	311
[35] Li_xHfNCl	0.16	0.5663[c]	1	1	1	1.56	2.6906 [1s, 2.6906]	331
[36] Na_xHfNCl	0.18	0.3259	1	1	1	1.85	6.8018 [2p, 3.4009]	331
[33] Mg_xHfNCl	0.1	0.3548[c]	1	2	2	1.475	7.8258 [2p, 3.9129]	331
[37] Sr_xHfNCl	0.09	0.3364[c]	1	2	2	2.095	11.932 [4p, 2.9830]	331
[37] Ba_xHfNCl	0.1	0.3072[c]	1	2	2	2.34	14.800 [5p, 2.9601]	331
[38] K_xBP	0.2	0.2249	1	1	1	2.315	7.7256 [3p, 2.5752]	152
[38] Rb_xBP	0.2	0.1956	1	1	1	2.5	10.881 [4p, 2.7202]	152
[38] Cs_xBP	0.2	0.1851	1	1	1	2.815	13.651 [5p, 2.7302]	152
[38] Ca_xBP	0.1	0.2601[c]	1	2	2	1.87	8.6583 [3p, 2.8861]	152
[39] Pd_xHoTe_3	0.08	0.1204	1	9	10[b]	1.545	13.618 [4d, 3.4044]	465
[39] $Pd_xY_2Te_5$	0.08	0.1204	1	9	10[b]	1.545	13.618 [4d, 3.4044]	465

[a]Continued with a separate footnote. [b]N_{val} includes outer s and d electrons for transition metals. [c]Calculated concentration deviates considerably from the experimentally determined value, at $x_{calc.onset} \approx 3.5 \times x_{exp.onset}$. [d]No available detailed reports on efforts to obtain other concentrations.

is a transition metal. For alkali and alkaline-earth metal intercalates, $N_{val} = N_{ee}$. For example, potassium yields $N_{val} = N_{ee} = N_{ep} = 1$ and strontium yields $N_{val} = N_{ee} = 2$ and $N_{ep} = 1$.

The effective nuclear charge Z_{eff} seen by the innermost electron ($N_{ep} = 1$) can be calculated using eq 7.

$$Z_{eff} = \zeta \times n \tag{7}$$

where ζ is the orbital exponent[45,59] of the electron with principal quantum number n. In other words, Z_{eff} is the effective nuclear charge seen by a single outer electron after all other outer electrons of N_{ee} are first accounted for. For example, for oxygen, copper, strontium, and potassium intercalates, the right side of eq 7 is 2.2458 × 2 (N_{ee} = 5), 4.4002 × 3 (N_{ee} = 10), 2.9830 × 4 (N_{ee} = 2), and 2.5752 × 3 (N_{ee} = 1), respectively. These intercalates and their calculated Z_{eff} are explicitly shown in Table 3.

The dimensionless constant A_s was determined from eq 3 by the use of onset data from Cu_xTiSe_2.[8] This compound was chosen because it has the best resolution in dopant concentration as it evolves from an insulator to a super-

https://doi.org/10.1021/acsphyschemau.1c00027
ACS Phys. Chem Au 2022, 2, 108−117

conductor, leading to a more precise determination of the onset of superconductivity. For Cu_xTiSe_2, the variables are $N_{ep} = 1$, $N_{ee} = 10$, $R = 1.4$ Å, $Z_{eff} = 13.201$, $V_{unit} = 65$ Å^3, $P = 101,325$ Pa, and the experimentally measured onset concentration, $x_{exp.onset} = 0.045$. As a result, the constant A_s is equal to 4.01×10^{-5}.

Mechanical equilibrium for all intercalated compounds mentioned in this report was maintained before and during measurement of T_c. Specifically, the sample pressure and volume remained unchanged, precisely at 1 atm. Using eq 3, the superconducting onset concentration $x_{calc.onset}$ is calculated and compared to the experimentally measured value, $x_{exp.onset}$, for other intercalated insulators; these values are displayed in Tables 3 and 4. Table 5 contains lattice parameters used in the calculation for $x_{calc.onset}$. Surprisingly, eq 3 reasonably estimates the concentration x at the onset of superconductivity for many of the intercalated insulators mentioned in the report. This is shown graphically in Figure 4, where the data clustering on or near the green region reveals the most successful prediction of onset concentrations, $x_{calc.onset}/x_{exp.onset} = 1 \pm 20\%$. Due to the simple yet intricate form of eq 3, the near exact estimation of onset concentrations, in terms of physical parameters of the host and intercalate, indicates the possibility of a coincidence to be unlikely. However, other ideas are required to be posed and tested to verify this suspicion.

Table 5. Lattice Parameters of Insulators Mentioned in Table 3 [(Element)$_y$(Insulator)] for All 39 Compounds Listed in Tables 3 and 4

insulator (lattice constants)	a (Å)	b (Å)	c (Å)
$TiSe_2$	3.54	3.54	6.01
$IrTe_2$	3.99	3.99	5.47
Bi_2Se_3	4.142	4.142	29.83
C_{60}	14.154	14.154	14.154
$[Na_{0.3}]MoS_2$	~3.20	~3.20	14.97
$[K_{0.13}]MoS_2$	3.212	3.212	15.871
$[Rb_{0.3}]MoS_2$	3.2039	3.2039	17.1937
$[Cs_{0.3}]MoS_2$	~3.20	~3.20	19.61
$[(Ca, Sr, Ba)_{0.2}]MoS_2$	~3.20	~3.20	18.64
$C_{22}H_{14}$	8.427	6.17	13.548
$C_{14}H_{10}$	8.43	6.134	9.417
YBCO	3.82	3.885	11.683
ZrNCl	3.604	3.604	27.672
HfNCl	3.589	3.589	29.722
BP (black phosphorus)	3.31	10.48	4.37
$HoTe_3$	4.286	25.304	4.288
Y_2Te_5	4.286	25.304	4.288

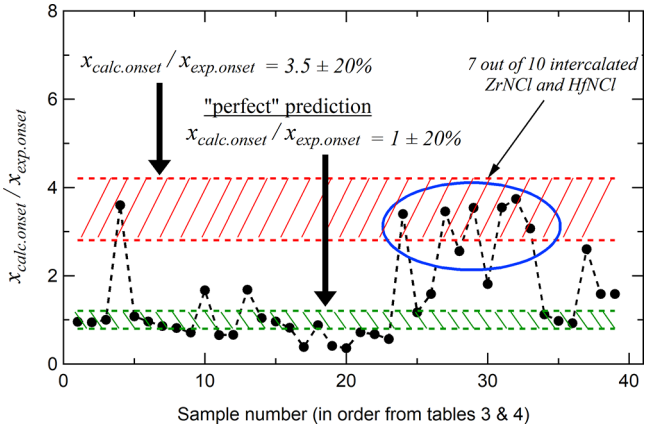

Figure 4. Ratio between $x_{calc.onset}$ and $x_{exp.onset}$ for all 39 intercalated compounds listed in Tables 3 and 4. The green region represents a "perfect" prediction between experimentally verified $x_{exp.onset}$ and $x_{calc.onset}$ calculated from eq 3, resulting in a ratio of $x_{calc.onset}/x_{exp.onset} = 1 \pm 20\%$. The red region represents $x_{calc.onset}/x_{exp.onset} = 3.5 \pm 20\%$.

$$T_{c\text{-}calc} = A_s \times \left| \frac{N_{ep}E_{ep} + N_{ee} \times (E_{ee} - E_{fermi})}{N_{val}K_B} \right| \quad (8)$$

Combining eqs 1 and 3 leads to eq 8 for calculating transition temperatures at x_{onset} as a function of x, N_{val}, N_{ep}, N_{ee}, R, Z_{eff}, V_{unit}, and A_s. See the Supporting Information, where eq 8 is evaluated for superconducting compounds with experimentally verified temperature phase diagrams: Cu_xTiSe_2, $Alkali_3C_{60}$ (alkali = K, Rb, Cs), and $YBa_2Cu_3O_{6+x}$. Equation 8 does not exactly reproduce phase diagrams because it was derived for onset conditions; however, concentrations of $x \geq x_{onset}$ closely approximate some as shown in plots S1, S2, and S3 in the Supporting Information.

Pressure Dependence, $P > 1$ atm

In the first section, it was shown that in the limit of small x, for dT_c/dx at $P = 1$ atm, the ideal gas equation can be used to characterize the onset of superconductivity in intercalated insulators, such that $(PV)/(x_{onset}N_{val}K_BT_c) = 1$. In comparison, available reports on the pressure dependence on T_c for intercalated insulators crossing the insulator−superconductor boundary do not exist in abundance. However, at least one report suggests a violation of the ideal gas law equation in the limit of "small P", for dT_c/dP at x = constant. For the intercalated A15 structure of Cs_3C_{60}, superconductivity first occurs at $P_{onset} = 4440$ atm.[10] At the onset, $V_{unit} = 1585$ Å and $T_c = 35$ K. This leads to the ratio $(P_{onset}V)/(xN_{val}K_BT_c) = 1312$, an apparent violation of the ideal gas equation by a factor of 10^3. The ratio is between 0.67 and 1 for the intercalated fcc structure of Cs_3C_{60}, for dT_c/dx at $P = 1$ atm.

There are several possible reasons for the large ratio estimated for the A15 structure. Maybe the valence electron of the intercalate, Cs_3, can no longer be used to characterize the onset for dT_c/dP, or maybe it can, but its contribution is greatly diminished by a factor of 10^3. The ideal gas law relation may also be irrelevant for dT_c/dP, or most likely, it is only relevant in the limit of low concentrations x and low pressures near 1 atm. More data for intercalated superconductors at elevated pressures are needed to elucidate this matter.

DISCUSSION

It is clear that when provided with basic information of the intercalate and its host environment, as shown above, it is possible to estimate the minimum intercalate concentration required to induce superconductivity within insulators. Even though this appears true in general, concentration estimates for 7 out of 10 intercalated ZrNCl and HfNCl are 3−3.5 times higher than values determined from experiment, as shown in Figure 4. Therefore, although the ideal gas law equation can be used to characterize their onset transition temperatures, the final formula deduced from it does not accurately predict onset concentrations. It is worth mentioning ZrNCl and HfNCl are the only insulators in this report, which contain superconducting binary constituents: they are ZrN[60] and HfN,[61] respectively. Also, while the above sections neglect interactions between the intercalate and the host, the superconductivity in ZrNCl and

https://doi.org/10.1021/acsphyschemau.1c00027
ACS Phys. Chem Au 2022, 2, 108−117

HfNCl is thought to be dominated by such interactions. For example, upon lithium intercalation of ZrNCl, it is believed that the compound becomes metallic by partially filling the t_{2g} band. This occurs because electrons are transferred from lithium to ZrN layers through chlorine layers.[60] Therefore, the dominant interaction in intercalated ZrNCl and perhaps in HfNCl seems to occur primarily between the intercalate and the binary components of the host compound (e.g., ZrN and HfN), thereby causing the estimation of onset parameters to depend on intercalate−host interactions for ZrNCl and HfNCl.

Because the isotope effect is one of the few hallmarks of superconductivity, it was surprising to empirically observe T_c independent of isotopic mass (i.e., ideal gas) at the insulator-superconductor boundary for intercalates. This mass independence is also evident in the final equation derived to predict onset concentrations. Though unexpected, the absence of the isotope effect was shown experimentally via magnetization and resistivity measurements for alkali intercalated C_{60}, when ^{85}Rb was substituted for ^{87}Rb.[62−64] Seeing that the experimental perturbation occurred with the intercalate (while closely obeying onset conditions) and not the host, the isotope effect can be modeled similar to previous sections by eq 9, the energy due to electron−neutron interactions among intercalates. In terms of resistivity measurements, for example, charged current densities would create a magnetic field, $\nabla \times B_J = \mu_o J$. These fields would then interact with the magnetic moments of nearby intercalate neutrons ($\mu_n = -1.91 \times N_n \mu_N$),[65] where N_n is the number of neutrons in the intercalate and mp is the proton mass in eq 10. For typical electron densities used for measuring transition temperatures via resistivity, $J \sim 10-100$ mA/cm^2,[48] the effect on T_c is confirmed negligible because $(E_{ep} + E_{ee})/E_{en} \approx 10^{11}$ for K_3C_{60} and Rb_3C_{60}.

$$E_{en} = -N_n \times (-1.91 \times \mu_N)\cdot(B_J) \tag{9}$$

$$\mu_N = \frac{e\hbar}{2m_p} \tag{10}$$

With further verification, the procedure outlined in this article can be seen as an empirical blueprint for creating new superconductors from insulators, and perhaps low-density semimetals. For example, suppose one desires to synthesize a new superconducting intercalate, Al_xC_{60}, eq 3 suggests it would require a concentration of around $x = 0.8$. According to eq 1, the projected onset T_c for $Al_{0.8}C_{60}$ would be 6.5 K. This applies to $Al_{n+x}C_{60}$ as well, where n = integer, if Al_nC_{60} were found to be insulating with comparable lattice parameters to C_{60}. Keep in mind that solving eq 3 seems to reveal possibilities of new superconductors; it does not govern the chemical or thermodynamic stability of the desired new superconducting compound. Therefore, creating new intercalated compounds such as $Al_{n+0.8}C_{60}$ may not be possible when other parameters are examined, such as the dopant's solubility and diameter.

Much work is needed to improve the accuracy in predicting onset concentrations; Figure 4 indicates the necessity. To accomplish this, currently, the influences of spin and intercalate−host interactions are being considered. Other empirically motivated forms of intercalate−intercalate interactions are also being considered and the influence of external perturbations (e.g., magnetic fields and pressure) will follow. To this end, in light of the current observation that the ideal gas law relation describes the insulator−superconductor boundary for intercalated insulators, for better predictions, a rigorous approach guided by first principles may prove beneficial.

CONCLUSIONS

The insulator−superconductor boundary of intercalated insulators can be modeled almost exactly using the ideal gas law equation. This empirical observation leads to certain assumptions about intercalated systems, which aid in predicting onset concentrations required to bring about superconductivity in insulators. Predictions seem possible when basic information of the intercalate (e.g., atomic radius) and its environment (e.g., lattice parameters) is known beforehand.

ASSOCIATED CONTENT

Supporting Information

The Supporting Information is available free of charge at https://pubs.acs.org/doi/10.1021/acsphyschemau.1c00027.

Estimated phase diagrams for superconductivity in Cu_xTiSe_2 and $YBa_2Cu_3O_{6+x}$ and estimated boundary and phase diagram for superconductivity at $x = 1$ in $A_{2+x}C_{60}$ (A = Na, K, Rb, and Cs) (PDF)

AUTHOR INFORMATION

Corresponding Author

Shermane M. Benjamin − *Physics Department, Montana State University, Bozeman, Montana 59717-3840, United States;* orcid.org/0000-0003-0594-7490; Email: sbenjamin21@gmail.com

Complete contact information is available at: https://pubs.acs.org/10.1021/acsphyschemau.1c00027

Notes

The author declares no competing financial interest.

REFERENCES

(1) Kamerlingh Onnes, H. The superconductivity of mercury. *Commun. Phys. Lab. Univ. Leiden* **1911**, *122*, 122−124.
(2) Schmalian, J. Failed theories of superconductivity. *Mod. Phys. Lett. B* **2010**, *24*, 2679−2691.
(3) Matthias, B. T. Transition Temperatures of Superconductors. *Phys. Rev.* **1953**, *92*, 874−876.
(4) Matthias, B. T. Chapter V Superconductivity in the Periodic System. In *Progress in Low Temperature Physics*; Gorter, C. J., Ed.; Elsevier, 1957; Vol. *2*, pp 138−150.
(5) Matthias, B. T.; Geballe, T. H.; Compton, V. B. Superconductivity. *Reviews of Modern Physics* **1963**, *35*, 1−22.
(6) Stanev, V.; Oses, C.; Kusne, A. G.; Rodriguez, E.; Paglione, J.; Curtarolo, S.; Takeuchi, I. Machine learning modeling of superconducting critical temperature. *npj Comput. Mater.* **2018**, *4*, 29.
(7) Konno, T.; Kurokawa, H.; Nabeshima, F.; Sakishita, Y.; Ogawa, R.; Hosako, I.; Maeda, A. Deep learning model for finding new superconductors. *Phys. Rev. B* **2021**, *103*, 014509.
(8) Morosan, E.; Zandbergen, H. W.; Dennis, B. S.; Bos, J. W. G.; Onose, Y.; Klimczuk, T.; Ramirez, A. P.; Ong, N. P.; Cava, R. J. Superconductivity in CuxTiSe2. *Nat. Phys.* **2006**, *2*, 544−550.
(9) Takabayashi, Y.; Ganin, A. Y.; Jeglič, P.; Arčon, D.; Takano, T.; Iwasa, Y.; Ohishi, Y.; Takata, M.; Takeshita, N.; Prassides, K.; Rosseinsky, M. J. The Disorder-Free Non-BCS Superconductor Cs 3 C 60 Emerges from an Antiferromagnetic Insulator Parent State. *Science* **2009**, *323*, 1585−1590.
(10) Ganin, A. Y.; Takabayashi, Y.; Khimyak, Y. Z.; Margadonna, S.; Tamai, A.; Rosseinsky, M. J.; Prassides, K. Bulk superconductivity at 38 K in a molecular system. *Nat. Mater.* **2008**, *7*, 367−371.

(11) McCauley, J. P.; Zhu, Q.; Coustel, N.; Zhou, O.; Vaughan, G.; Idziak, S. H. J.; Fischer, J. E.; Tozer, S. W.; Groski, D. M. Synthesis, structure, and superconducting properties of single-phase Rb3C60. A new, convenient method for the preparation of M3C60 superconductors. *J. Am. Chem. Soc.* **1991**, *113*, 8537−8538.
(12) Liang, R.; Bonn, D. A.; Hardy, W. N. Evaluation ofCuO2plane hole doping inYBa2Cu3O6+xsingle crystals. *Phys. Rev. B* **2006**, *73*, 180505.
(13) Morosan, E.; Li, L.; Ong, N. P.; Cava, R. J. Anisotropic properties of the layered superconductorCu0.07TiSe2. *Phys. Rev. B: Condens. Matter Mater. Phys.* **2007**, *75*, 104505.
(14) Bardeen, J.; Cooper, L. N.; Schrieffer, J. R. Theory of Superconductivity. *Phys. Rev.* **1957**, *108*, 1175−1204.
(15) Shen, J.; He, W.-Y.; Yuan, N. F. Q.; Huang, Z.; Cho, C.-w.; Lee, S. H.; Hor, Y. S.; Law, K. T.; Lortz, R. Nematic topological superconducting phase in Nb-doped Bi_2Se_3. *npj Comput. Mater.* **2017**, *2*, 59.
(16) Morosan, E.; Wagner, K. E.; Zhao, L. L.; Hor, Y.; Williams, A. J.; Tao, J.; Zhu, Y.; Cava, R. J. Multiple electronic transitions and superconductivity in Pd_xTiSe_2. *Phys. Rev. B* **2010**, *81*, 094524.
(17) Kamitani, M.; Bahramy, M. S.; Arita, R.; Seki, S.; Arima, T.; Tokura, Y.; Ishiwata, S. Superconductivity in CuxIrTe2driven by interlayer hybridization. *Phys. Rev. B* **2013**, *87*, 180501.
(18) Smylie, M. P.; Willa, K.; Claus, H.; Koshelev, A. E.; Song, K. W.; Kwok, W.-K.; Islam, Z.; Gu, G. D.; Schneeloch, J. A.; Zhong, R. D.; Welp, U. Superconducting and normal-state anisotropy of the doped topological insulator Sr0.1Bi2Se3. *Sci. Rep.* **2018**, *8*, 7666.
(19) Kondo, R.; Yoshinaka, T.; Imai, Y.; Maeda, A. Reproducible Synthetic Method for the Topological Superconductor CuxBi2Se3. *J. Phys. Soc. Jpn.* **2013**, *82*, 063702.
(20) Holczer, K.; Klein, O.; Grüner, G.; Thompson, J. D.; Diederich, F.; Whetten, R. L. Critical magnetic fields in the superconducting state ofK3C60. *Phys. Rev. Lett.* **1991**, *67*, 271−274.
(21) Irons, S. H.; Liu, J. Z.; Klavins, P.; Shelton, R. N. Magnetic properties of superconductingK3C60andRb3C60synthesized from large single-crystal fullerenes. *Phys. Rev. B* **1995**, *52*, 15517−15521.
(22) Ihara, Y.; Alloul, H.; Wzietek, P.; Pontiroli, D.; Mazzani, M.; Riccò, M. NMR Study of the Mott Transitions to Superconductivity in the TwoCs3C60Phases. *Phys. Rev. Lett.* **2010**, *104*, 256402.
(23) Woollam, J. A.; Somoano, R. B. Physics and chemistry of MoS2 intercalation compounds. *Mater. Sci. Eng.* **1977**, *31*, 289−295.
(24) Andersen, A.; Kathmann, S. M.; Lilga, M. A.; Albrecht, K. O.; Hallen, R. T.; Mei, D. First-Principles Characterization of Potassium Intercalation in Hexagonal 2H-MoS2. *J. Phys. Chem. C* **2012**, *116*, 1826−1832.
(25) Zhang, R.; Tsai, I.-L.; Chapman, J.; Khestanova, E.; Waters, J.; Grigorieva, I. V. Superconductivity in Potassium-Doped Metallic Polymorphs of MoS2. *Nano Lett.* **2016**, *16*, 629−636.
(26) Somoano, R. B.; Hadek, V.; Rembaum, A. Alkali metal intercalates of molybdenum disulfide. *J. Chem. Phys.* **1973**, *58*, 697−701.
(27) Rao, G. V. S.; Shafer, M. W.; Kawarazaki, S.; Toxen, A. M. Superconductivity in alkaline earth metal and Yb intercalated group VI layered dichalcogenides. *J. Solid State Chem.* **1974**, *9*, 323−329.
(28) Mitsuhashi, R.; Suzuki, Y.; Yamanari, Y.; Mitamura, H.; Kambe, T.; Ikeda, N.; Okamoto, H.; Fujiwara, A.; Yamaji, M.; Kawasaki, N.; Maniwa, Y.; Kubozono, Y. Superconductivity in alkali-metal-doped picene. *Nature* **2010**, *464*, 76−79.
(29) Kubozono, Y.; et al. Metal-intercalated aromatic hydrocarbons: a new class of carbon-based superconductors. *Phys. Chem. Chem. Phys.* **2011**, *13*, 16476−16493.
(30) Wang, X. F.; Liu, R. H.; Gui, Z.; Xie, Y. L.; Yan, Y. J.; Ying, J. J.; Luo, X. G.; Chen, X. H. Superconductivity at 5 K in alkali-metal-doped phenanthrene. *Nat. Commun.* **2011**, *2*, 507.
(31) Wang, X. F.; Yan, Y. J.; Gui, Z.; Liu, R. H.; Ying, J. J.; Luo, X. G.; Chen, X. H. Superconductivity inA1.5phenanthrene (A=Sr,Ba). *Phys. Rev. B* **2011**, *84*, 214523.
(32) Kawaji, H.; Hotehama, K.-i.; Yamanaka, S. Superconductivity of Alkali Metal Intercalated β-Zirconium Nitride Chloride, AxZrNCl (A = Li, Na, K). *Chem. Mater.* **1997**, *9*, 2127−2130.
(33) Yagyu, H.; Kato, M.; Tezuka, H.; Noji, T.; Yamanaka, S.; Koike, Y. A new family of superconducting intercalation compound of MgMNCl (M= Zr, Hf). *Phys. C* **2010**, *470*, S760−S761.
(34) Arroyo y de Dompablo, M. E.; Morán, E.; Alario-Franco, M. Á.; Drymiotis, F.; Bianchi, A. D.; Fisk, Z. Novel superconductors obtained by electrochemical Zn intercalation of β-ZrNCl and related compounds. *Int. J. Inorg. Mater.* **2000**, *2*, 581−588.
(35) Takano, T.; Kishiume, T.; Taguchi, Y.; Iwasa, Y. Interlayer-Spacing Dependence ofTcinLixMyHfNCl(M: Molecule) Superconductors. *Phys. Rev. Lett.* **2008**, *100*, 247005.
(36) Shamoto, S.-i.; Takeuchi, K.; Yamanaka, S.; Kajitani, T. Structural Study on NaxHfNCl System. *Phys. C* **2004**, *402*, 283−292.
(37) Zhang, S.; Tanaka, M.; Zhu, H.; Yamanaka, S. Superconductivity of layered β-HfNCl with varying electron-doping concentrations and interlayer spacings. *Supercond. Sci. Technol.* **2013**, *26*, 085015.
(38) Zhang, R.; Waters, J.; Geim, A. K.; Grigorieva, I. V. Intercalant-independent transition temperature in superconducting black phosphorus. *Nat. Commun.* **2017**, *8*, 15036.
(39) He, J. B.; Wang, P. P.; Yang, H. X.; Long, Y. J.; Zhao, L. X.; Ma, C.; Yang, M.; Wang, D. M.; Shangguan, X. C.; Xue, M. Q.; Zhang, P.; Ren, Z. A.; Li, J. Q.; Liu, W. M.; Chen, G. F. Superconductivity in Pd-intercalated charge-density-wave rare earth poly-tellurides RETen. *Supercond. Sci. Technol.* **2016**, *29*, 065018.
(40) Müller-Warmuth, W.; Schollhorn, R. *Progress in Intercalation Research*; Springer Science & Business Media, 2012.
(41) Saadaoui, H.; Salman, Z.; Luetkens, H.; Prokscha, T.; Suter, A.; MacFarlane, W. A.; Jiang, Y.; Jin, K.; Greene, R. L.; Morenzoni, E.; Kiefl, R. F. The phase diagram of electron-doped La2−xCexCuO4−δ. *Nat. Commun.* **2015**, *6*, 6041.
(42) Cooper, L. N. Bound Electron Pairs in a Degenerate Fermi Gas. *Phys. Rev.* **1956**, *104*, 1189−1190.
(43) Kittel, C. *Introduction to Solid State Physics*; Wiley, 1986.
(44) Slater, J. C. Atomic Radii in Crystals. *J. Chem. Phys.* **1964**, *41*, 3199−3204.
(45) Clementi, E.; Raimondi, D. L.; Reinhardt, W. P. Atomic Screening Constants from SCF Functions. II. Atoms with 37 to 86 Electrons. *J. Chem. Phys.* **1967**, *47*, 1300−1307.
(46) Benjamin, S. M.; Rieders, N. F.; Smith, M. G.; Neumeier, J. J. From Ta2S5 Wires to Ta2O5 and Ta2O5-xSx. *ACS Omega* **2021**, *6*, 5445−5450.
(47) Benjamin, S. M.; Smith, M. G.; Neumeier, J. J. Superconductivity in MgTa2S5. *Phys. C* **2021**, *591*, 1353966.
(48) Drenner, A. K.; Benjamin, S. M.; Smith, M. G.; Neumeier, J. J. Physical properties and superconductivity of SrTa2S5. *Phys. C* **2019**, *556*, 19−23.
(49) Drenner, A. K.; Benjamin, S. M.; Smith, M. G.; Neumeier, J. J. Physical properties and superconductivity of BaTa2S5. *Phys. C* **2019**, *566*, 1353522.
(50) Kulbachinskii, V.; Bulychev, B.; Kytin, V.; Krechetov, A.; Tarasov, V.; Konstanti- nova, E.; Velikodnyi, Y.; Muravlev, Y.; Zoteev, A. Magnetic and structural anomalies of Na_nC60 (n = 2, 3). *Open Phys.* **2010**, *8*, 101−112.
(51) Andersen, A.; Kathmann, S. M.; Lilga, M. A.; Albrecht, K. O.; Hallen, R. T.; Mei, D. First-Principles Characterization of Potassium Intercalation in Hexagonal 2H-MoS2. *J. Phys. Chem. C* **2012**, *116*, 1826.
(52) Nagata, S.; Aochi, T.; Abe, T.; Ebisu, S.; Hagino, T.; Seki, Y.; Tsutsumi, K. Superconductivity in the layered compound 2H-TaS2. *J. Phys. Chem. Solids* **1992**, *53*, 1259−1263.
(53) Lerf, A.; Sernetz, F.; Biberacher, W.; Schöllhorn, R. Superconductivity in layered ternary chalcogenides AxTaS2 and AxNbS2 and influence of topotactic solvation. *Mater. Res. Bull.* **1979**, *14*, 797−805.
(54) Tarascon, J. M.; Hull, G. W.; Waszczak, J. V. Synthesis, structural and physical properties of the binary molybdenum chalcogenide phase Mo15Se19 and of the related compounds M2Mo15Se19 and M3Mo15Se19 (M=group 1A metal; Sn,Pb;Cd). *Mater. Res. Bull.* **1985**, *20*, 935−946.
(55) Evans, M. J.; Wu, Y.; Kranak, V. F.; Newman, N.; Reller, A.; Garcia-Garcia, F. J.; Häussermann, U. Structural properties and superconductivity in the ternary inter- metallic compounds MAB

https://doi.org/10.1021/acsphyschemau.1c00027
ACS Phys. Chem Au 2022, 2, 108−117

($M=\\text{Ca}$, Sr, Ba; $A=\\text{Al}$, Ga, In; $B=\\text{Si}$, Ge, Sn). *Phys. Rev. B* **2009**, *80*, 064514.
(56) Matthias, B. T.; Hulm, J. K. A Search for New Superconducting Compounds. *Phys. Rev.* **1952**, *87*, 799−806.
(57) Kushwaha, S. K.; Krizan, J. W.; Xiong, J.; Klimczuk, T.; Gibson, Q. D.; Liang, T.; Ong, N. P.; Cava, R. J. Superconducting properties and electronic structure of NaBi. *J. Phys.: Condens. Matter* **2014**, *26*, 212201.
(58) Pines, D. Electron Interaction in Metals. In *Solid State Physics*; Seitz, F., Turnbull, D., Eds.; Academic Press, 1955; Vol. *1*, pp 367−450.
(59) Clementi, E.; Raimondi, D. L. Atomic Screening Constants from SCF Functions. *J. Chem. Phys.* **1963**, *38*, 2686−2689.
(60) Yamanaka, S.; Kawaji, H.; Hotehama, K.-i.; Ohashi, M. A new layer-structured nitride superconductor. Lithium-intercalated ?-zirconium nitride chloride, LixZrNCl. *Adv. Mater.* **1996**, *8*, 771−774.
(61) Hulm, J. K.; Walker, M. S.; Pessall, N. High Tc-experimental achievement. *Physica* **1971**, *55*, 60−68.
(62) Ebbesen, T. W.; Tsai, J. S.; Tanigaki, K.; Hiura, H.; Shimakawa, Y.; Kubo, Y.; Hirosawa, I.; Mizuki, J. Dopant isotope effect on superconductivity in Rb3C60. *Phys. C* **1992**, *203*, 163−166.
(63) Burk, B.; Crespi, V. H.; Fuhrer, M. S.; Zettl, A.; Cohen, M. L. Alkali-metal isotope effect in Rb3C60. *Phys. C* **1994**, *235−240*, 2493−2494.
(64) Burk, B.; Crespi, V. H.; Zettl, A.; Cohen, M. L. Rubidium isotope effect in superconductingRb3C60. *Phys. Rev. Lett.* **1994**, *72*, 3706−3709.
(65) Particle Data Group; et al. Review of Particle Physics. *Phys. Rev. D* **2012**, *86*, 010001.

NOTE ADDED AFTER ASAP PUBLICATION

This paper was published on the Web on November 16, 2021, with errors in the in-line equation prior to equation 9. The corrected version was reposted on November 22, 2021. Additional corrections were added, and the corrected version was reposted on November 24, 2021.

https://doi.org/10.1021/acsphyschemau.1c00027
ACS Phys. Chem Au 2022, 2, 108−117